

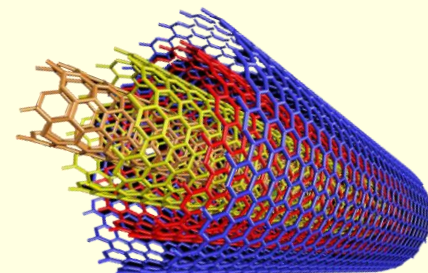
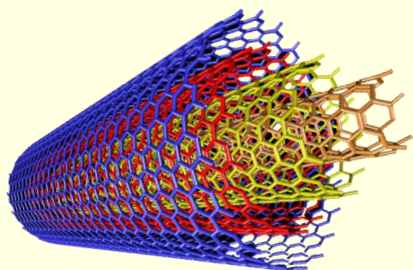
EXPANDED GRAPHITE, CARBON NANOTUBES AND ITS COMPOSITES

Yu. I. Sementsov⁽¹⁾ and S.L. Revo⁽²⁾

*⁽¹⁾Chuyko Institute of Surface Chemistry NAS Ukraine,
17 Generala Naumova str., Kyiv, 03164, Ukraine*

isc-sec@i12.com

*⁽²⁾Kyiv National University by Taras Shevchenko, Glushkov av. 2,
build.1, 03127 Kyiv, Ukraine*



Appearance of Expanded Graphite

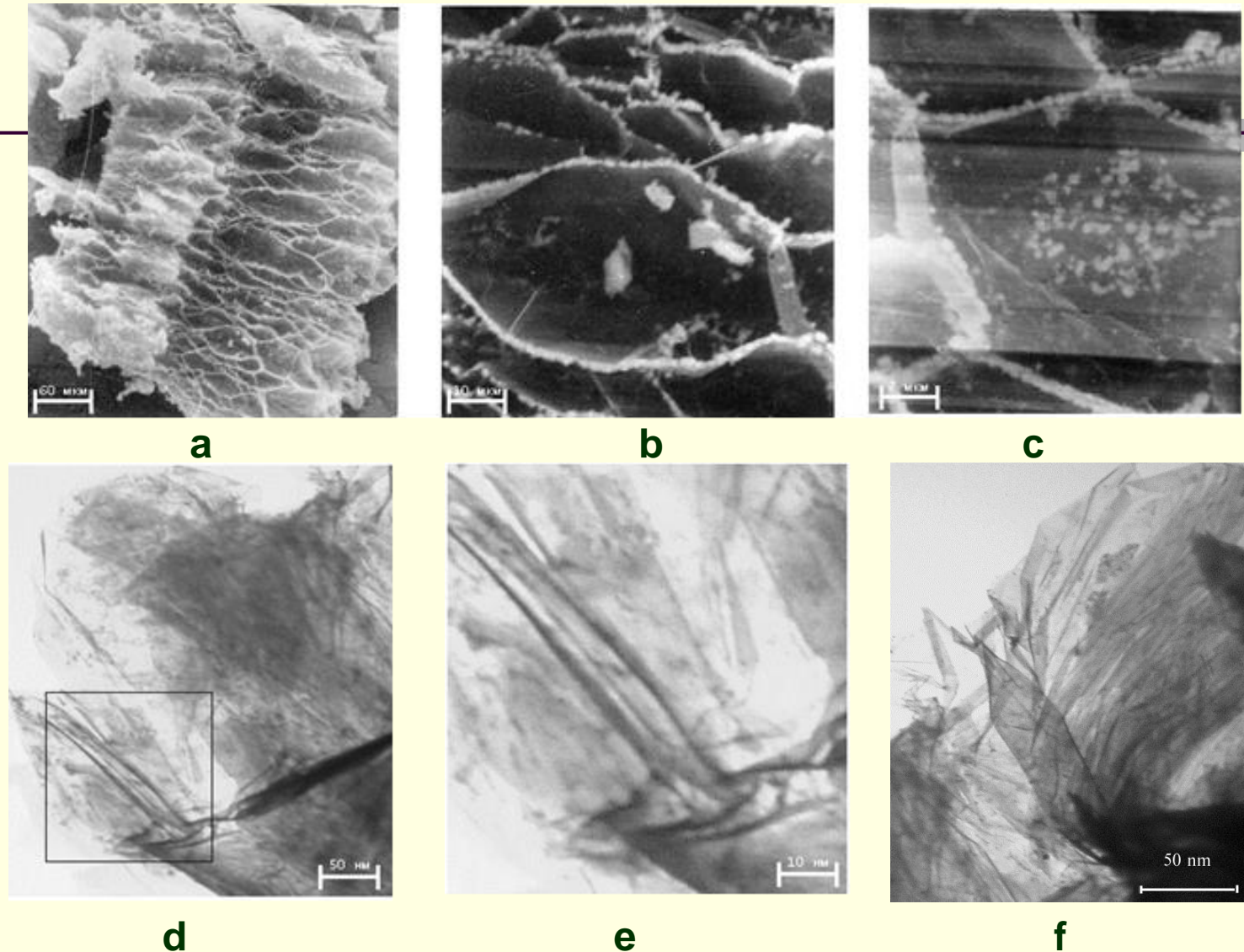
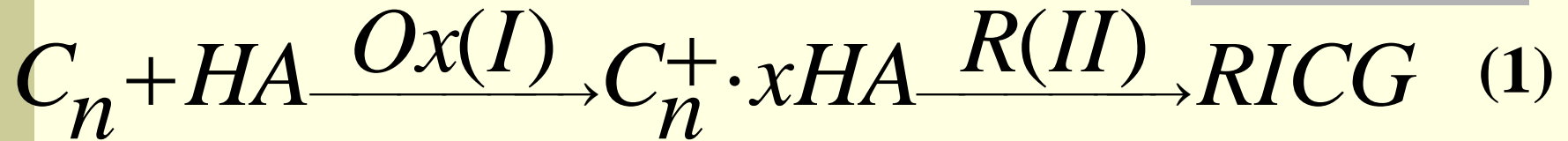


Fig. 1. Appearance of EG: a, b, c – scanning electron microscopy; d, e, f – transmission electron microscopy;

Expandable graphite

In basis of existent technologies of production of expandable intercalation compound of graphite (ICG) with Bronsted acids a next fundamental chart lies:



where: C_n – fragment of graphene's layer of graphite matrix; HA – Bronsted acids (for example: H_2SO_4 , HNO_3 , H_3PO_4); O_x – oxidizer (for example: HNO_3 , $K_2Cr_2O_7$, $KMnO_4$, $(NH_4)_2S_2O_8$, H_2O_2 , O_3 , CrO_3 , **electric current**); R – chemical agent (for example: H_2O , NH_4OH at alias); RICG – residual intercalation compound of graphite (RICG).

A process (I) is oxidization of graphite to produce ICG. A process (II) is a treatment of ICG to produce residual ICG. A process (II) is needed for stabilizing of the properties of ICG in time.

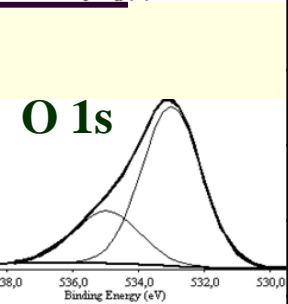
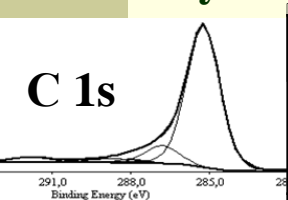
The structural features of EG and his properties are determined a structure of ICG (by the terms of process (I)), by the structure of product, leadthrough of process (II) got as a result, and by the terms of thermal decomposition.

For Example: The graphite structural parameters after some treatments

1	Material	d_{002} , nm	L_a , nm	L_c , nm
	Natural graphite	0,3354	110	40
	Expandable graphite	0,3355	65	10
	EG, hydrolyzed, $T_{HTT} = 400^\circ\text{C}$	0,3359	23	23
	EG, hydrolyzed, $T_{HTT} = 800^\circ\text{C}$	0,3360	21	22
	EG, hydrolyzed, $T_{HTT} = 1000^\circ\text{C}$	0,3356 – 0,3362	-	-
	EG, without hydrolysis, $T_{HTT} = 1800^\circ\text{C}$	0,338- 0,343	-	-

d_{002} - interlayer distance of graphite lattice and L_a and L_c sizes of coherent X-ray scattering area in the basal plane (L_a) and in the perpendicular direction (L_c)

X-ray Photoelectron High Resolution Spectra (structural state of the surface of graphite)



2	Samples	The total concentration of carbon, %	The relative concentration of carbon in the spectrum of C 1s, %				
			carbon of graphite	phenol, alcohol $E_b = 286,1-286,3$ eB (C-OH)	carbonyl, kinone $E_b = 287,3-287,6$ eB (C=O)	carboxyl, ether $E_b = 288,4-288,9$ eB (C-OOH)	$E_b = 290,4-290,8$ eB carbonate and/or adsorbed CO, CO ₂
	Expandable graphite, electrochemical	63,0	75,3	13,9	3,0	4,0	3,9
	Expandable graphite, chemical (NH ₄) ₂ S ₂ O ₈	78,0	80,9	11,6	3,0	2,4	2,1
	EG, electrochemical, 40 ampere-hour	86,5	81,0	10,0	2,1	3,4	3,6
	EG, electrochemical, 67 ampere-hour	97,7	83,6	10,5	2,9	0,9	2,1
	EG, electrochemical, 95% H ₂ SO ₄	97,6	83,9	16,1	±0	±0	±0
	EG, 1000°C, H ₂	97,5	87,8	12,2	±0	±0	±0

For Example:

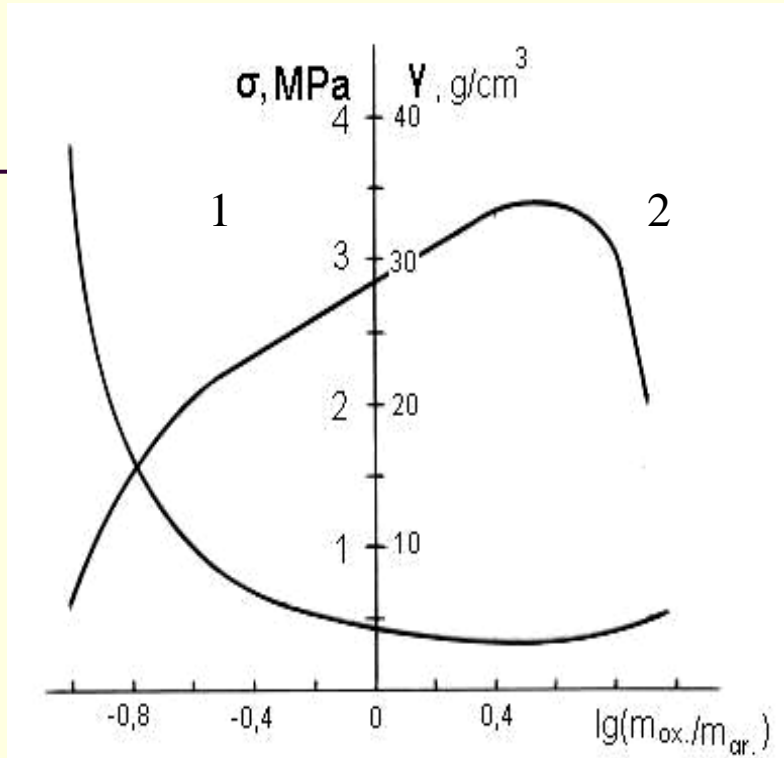


Fig. 2. The dependence bulk densities (γ) (1) and Limit Tensile Strength (σ) (2) of relations of mass oxidant to mass graphite ($\rho_{\text{sampl.}} = 0,9 \text{ g/cm}^3$, $m_{\text{ac.}} / m_{\text{gr.}} = 2$)

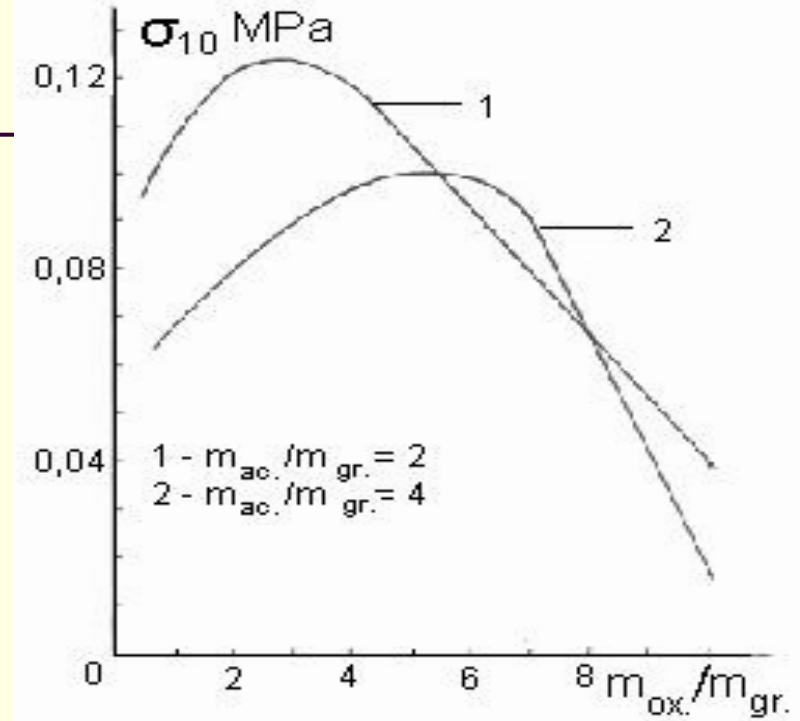
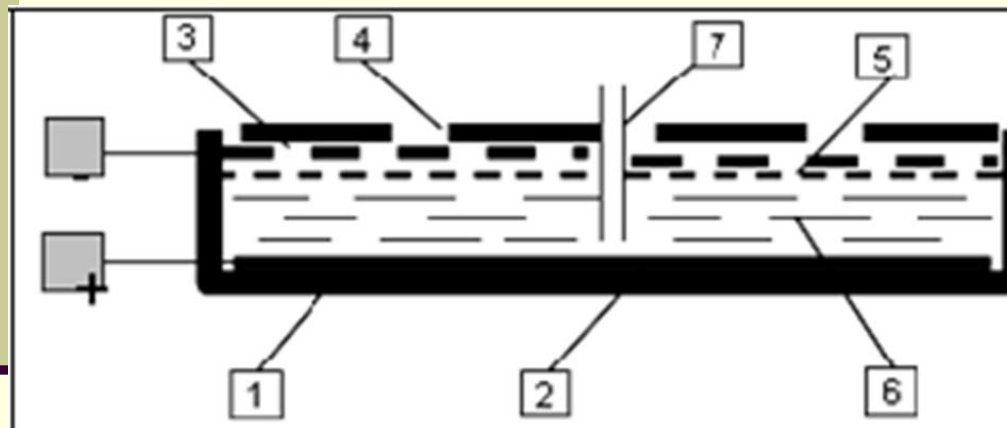


Fig. 3. The dependence of the compressive strength of the mass ratio of oxidizer to graphite ($\rho = 0,07 \text{ g/cm}^3$)

Technology of Expandable Graphite Production

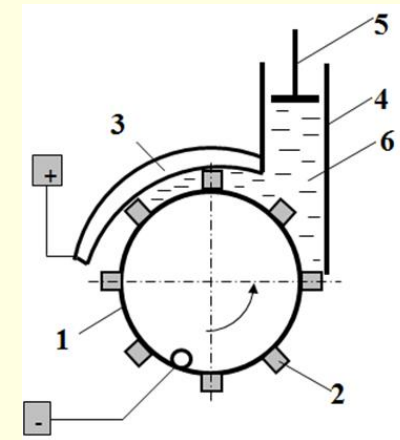
The constructions of electrochemical reactors for anodic oxidize of graphite (to obtain expandable graphite) are developed. Its capacity and economy is well-proven (on 1 kg of graphite is it needed 750 sm^3 50% sulphuric acid and $\sim 50 \text{ A}\cdot\text{h}$ electricity); the bulk density of EG was near 5 g/dm^3 and it was suitable for the production of sealing materials;

Fig. 4. Scheme of the horizontal-type reactor of periodic action



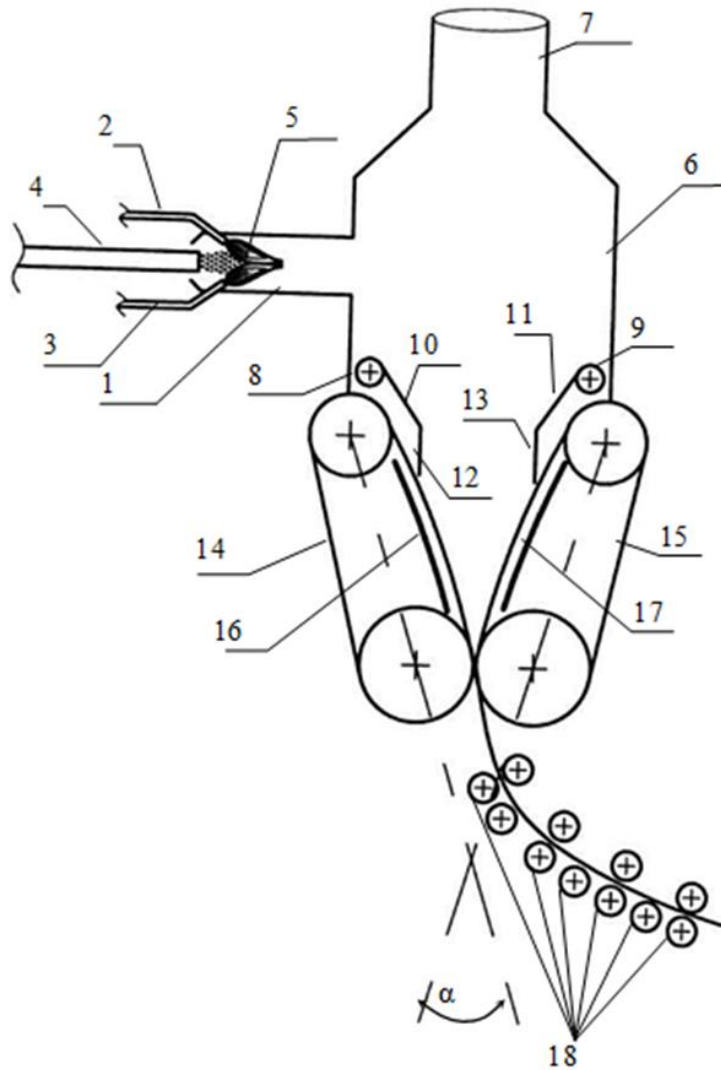
1 – housing; 2 – anode; 3 – separator;
4 – cathode; 5 – partition (membrane);
6 – graphite-acid mixture; 7 – drainage tube.

Fig. 5. Scheme of the drum-type reactor of continuous action



1 – drum cathode and separator;
2 – partition; 3 – folding plate anode;
4 – hopper; 5 – the piston;
6 – graphite-acid mixture

Fig. 6 .The Scheme of rolling mill for EG materials



1 – thermal shock chamber of expandable graphite;
 2,3 – gas burners; 4 – pipeline of air-graphite mixture;
 5 – area of heat treatment of expandable graphite; 6 – chamber with the union coupling (7): it is division of the exfoliated graphite and gaseous products; 8, 9 – drums; 10, 11 – limit band; 12, 13 – limit apron (plate); 14, 15 – bands of vertical transporter; 16, 17 – convex випуклі елементи deflected position device, відповідної криволінійної форми; 18 – roller bed (система валків); 19 – annealing oven; 20, 21 – горизонтальні horizontal transporters конвеєри; 22, 23 – калібрувальні size rolls валки; 24 – рухомий гільотинний moving guillotine пристрій; 25 – winding device пристрій для намотування фольги.

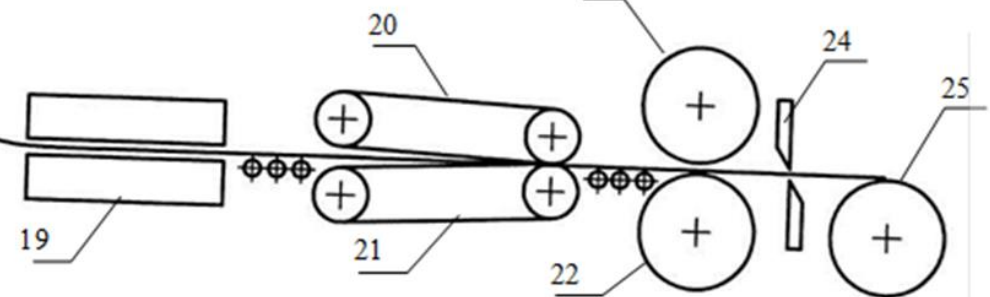


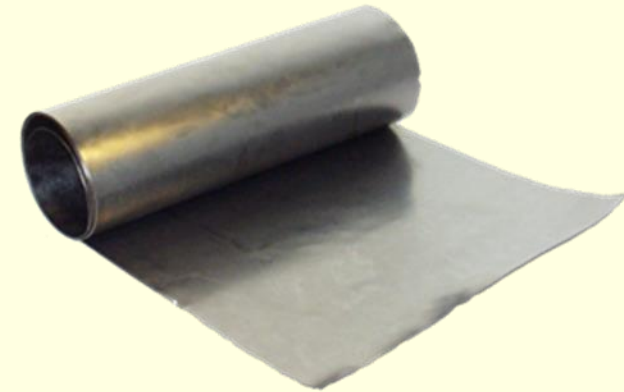
Fig. 7. Industrial Production of Exfoliated Graphite: Mechanicals Seals.



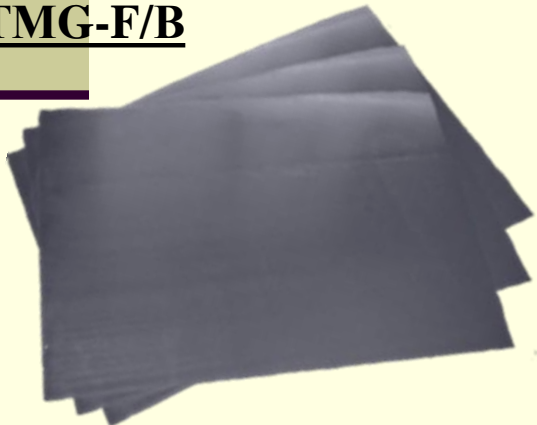
Sealing of high-pressure fittings with application of sealing ring TMG-F/B



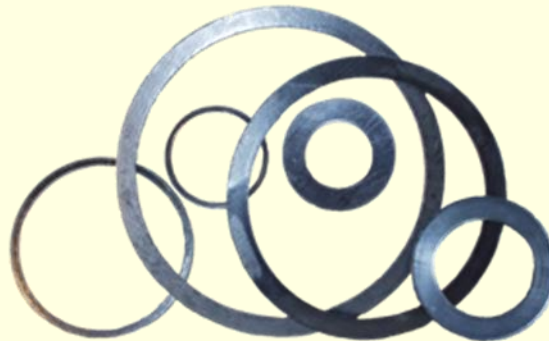
Braided Packing "TMG"



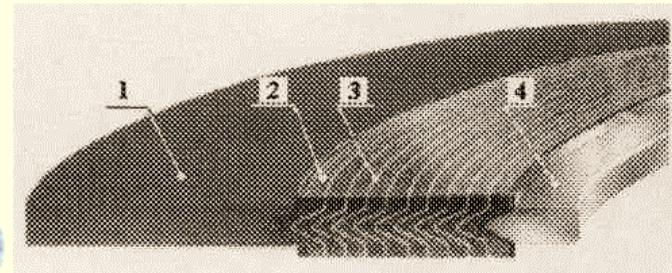
Graphite Foil "TMG"



Sheet material "TMG"



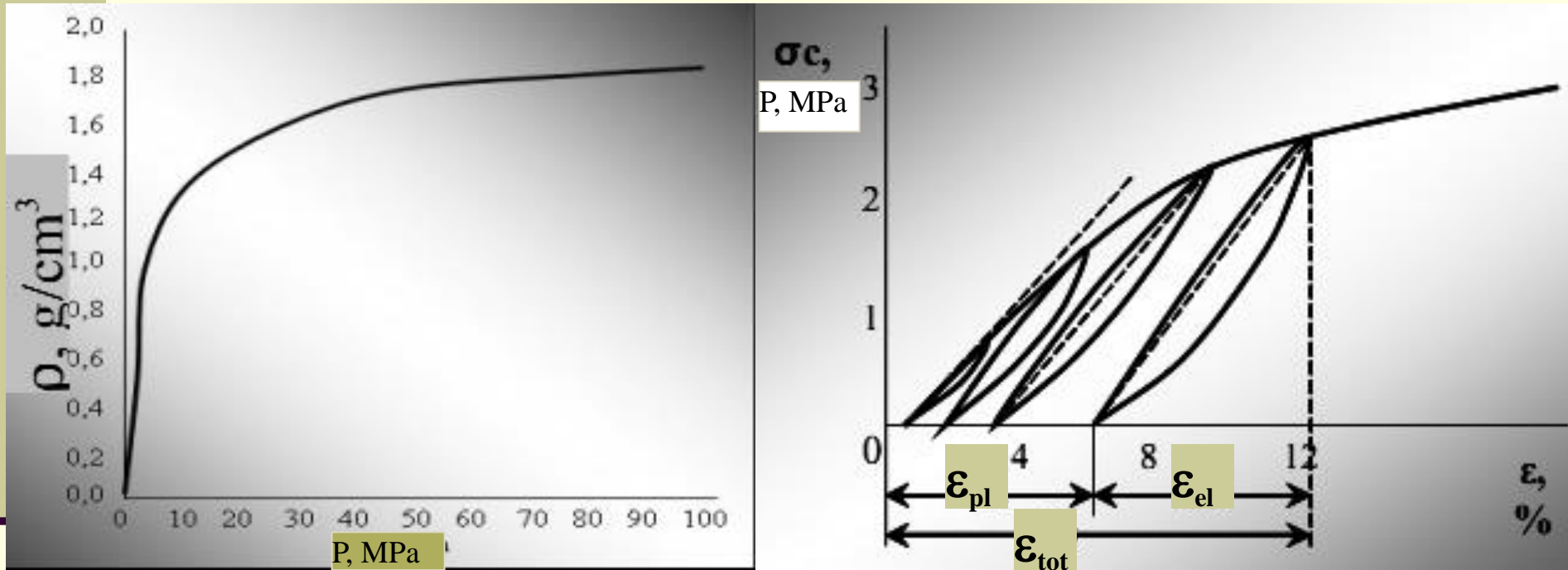
Graphite Gaskets "TMG"



Spiral winding sealing

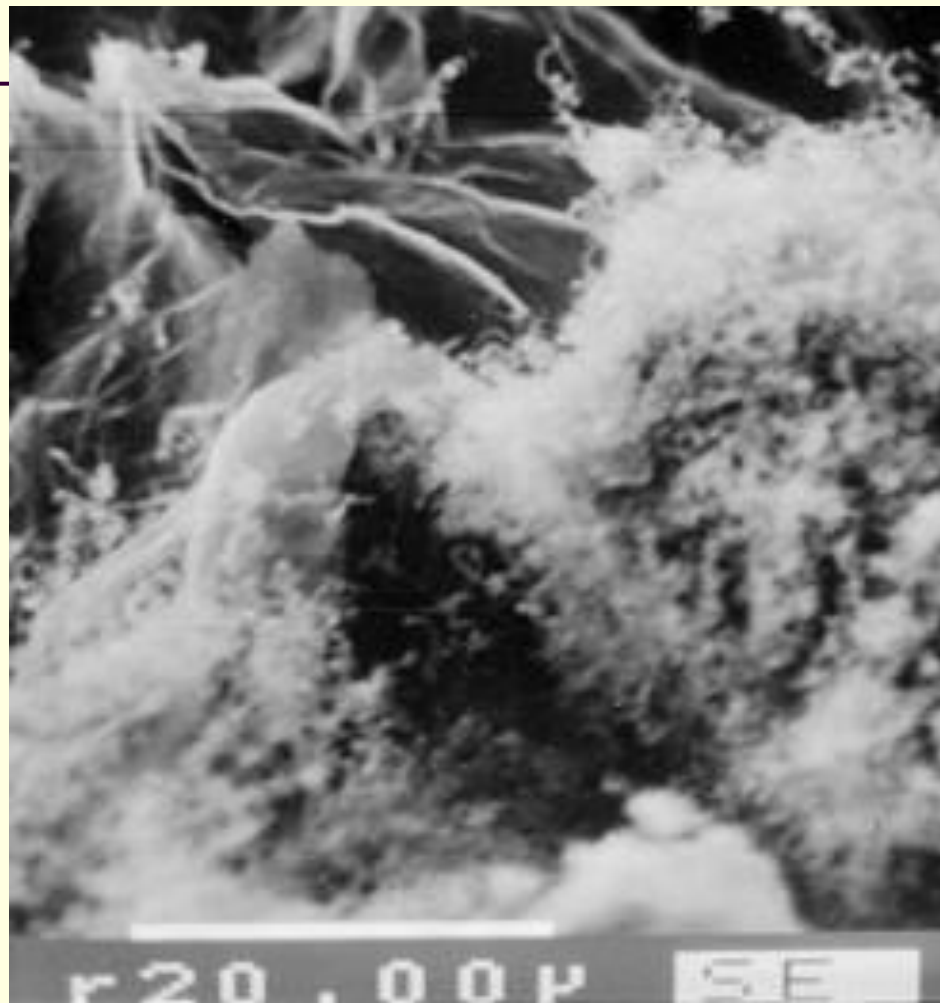
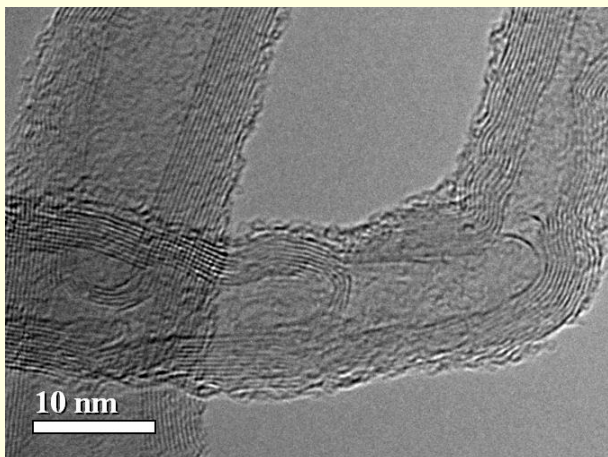
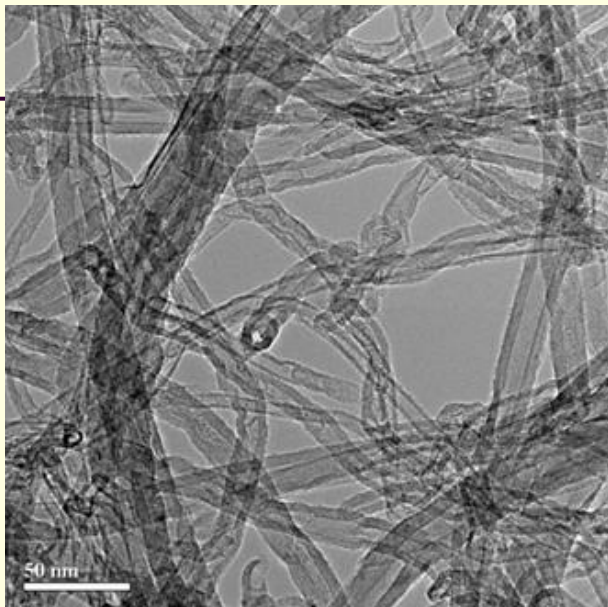
Fig. 8. EG:

left – dependence of density from compaction pressure;
right – compression diagram for repeated static loading



ϵ_{pl} – plasticity deformation; ϵ_{el} – elasticity deformation; ϵ_{tot} – total deformation

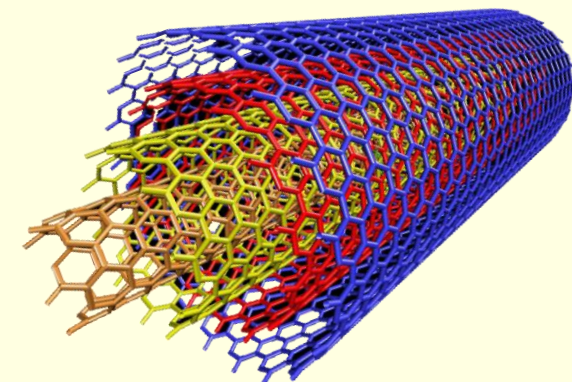
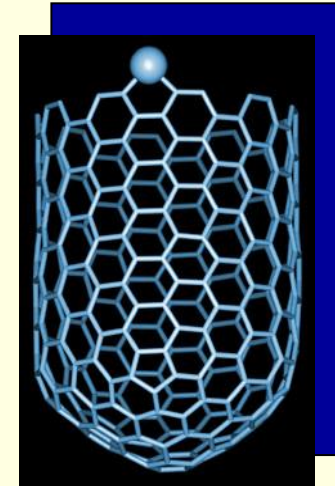
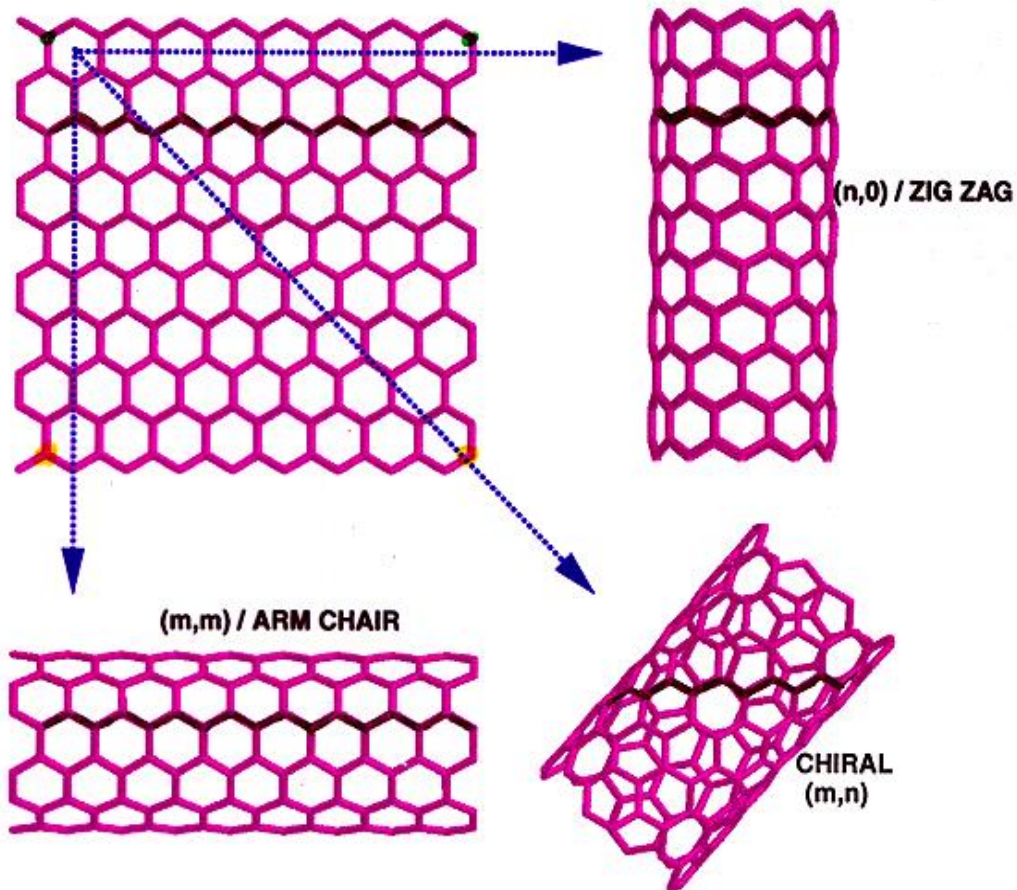
**Fig. 9. Multiwall carbon nanotubes and
EG /MWCNT composite**



Left – TEM of MWCNT; Right – SEM of composite EG/MWCNT;

Fig. 10. The scheme of the carbon nanotubes structure

- STRIP OF A GRAPHENE SHEET ROLLED INTO A TUBE

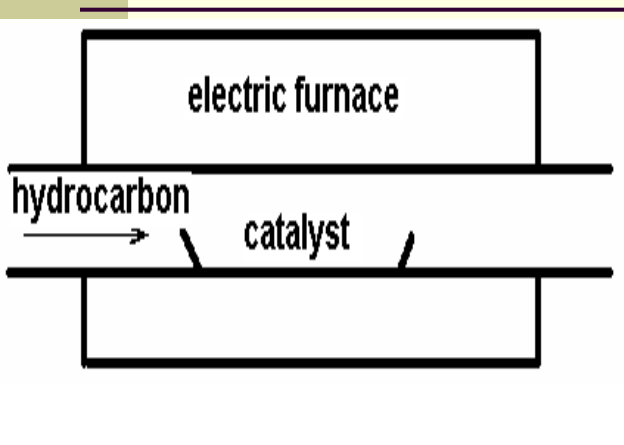


Comparison of CNTs Properties vs Other Reinforced Materials

Properties	CNTs	Compared materials	Value
Young's modulus	~1~1.8TPa	P-120 carbon fiber	840 GPa
		Aluminium borate whisker	392 GPa
Tensile strength (GPa)	~150	IM7carbon fiber	5.5
		Aluminium borate whisker	7.84
Electrical resistance ($\Omega \cdot \text{cm}$)	10^{-4}	Copper	1.7×10^{-6}
	10^{-6} (metallic)		
Thermal conductivity (W/mK)	~1200~3000	Diamond	700~2000

Aspect ration $\eta \geq 1\ 000$

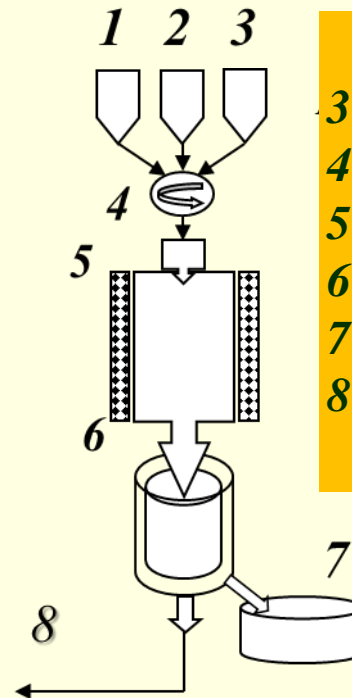
Fig. 11. Device of CNT Preparation by CVD Method



The principal scheme of device for CNT chemical preparation by precipitation from gas phase

Device for propylene catalytic pyrolysis with reactor volume 30 dm^3 and output about 1.5 kg per day

Fig. 12. Device of Catalyst Preparation to CVD Method of CNT Growth



- 3 - 1 container with salt solutions;
- 4 - mixer;
- 5 - electric furnace;
- 6 - electrostatic precipitator;
- 7 - vessel;
- 8 - water vapour

CERTIFICATE of QUALITY № _____

Number of lot __681____ Date «_20_» __march_____ 2009_года

The name of good: **Carbon nanotubes multiwalled (CNTMW)**Designation: **CNTMW TY Y 24.1-03291669-009:2009**Made in accordance with normative documentation **TY Y 24.1-03291669-009:2009**, and in accordance to established procedure**Description of Goods**

№ п/п	Parameters	Value, accordant to “TY Y”	Actual value
1	Quantity, kg		
2	Appearance	Light black powder. There is accepted a little admixture of loose aggregates, and inclusion of insignificant amount of white or yellow dots (the residue of not reacted catalyst)	
3	CNTMW structure	According customers requirements	Addendum 1
3	CNTMW bulk density g/dm ³	20-40	28
4	Mass content of ashes, %	Unpurified - 8-22 Purified - < 1,0	18,0
6	Specific surface of unpurified CNTMW, m ² /g	200-400	237
7	Specific surface CNTMW after acid purification, m ² /g	200-400	261
8	External diameter, nm	10-40	10-40
9	Specific electric resistance of unpurified CNTMW, Ohm cm	0,05-0,15	-
10	Specific electric resistance of pressed and purified from compounding material CNTMW, Ohm cm	0,05-0,10	-
11	The temperature of 5% mass loss after purification from compounding material	520-620	545

Conclusion of Control quality Department: CNTMW are in conform to normative documentation “TY Y”

Fig 13. Spectral characteristics of multiwall CNT

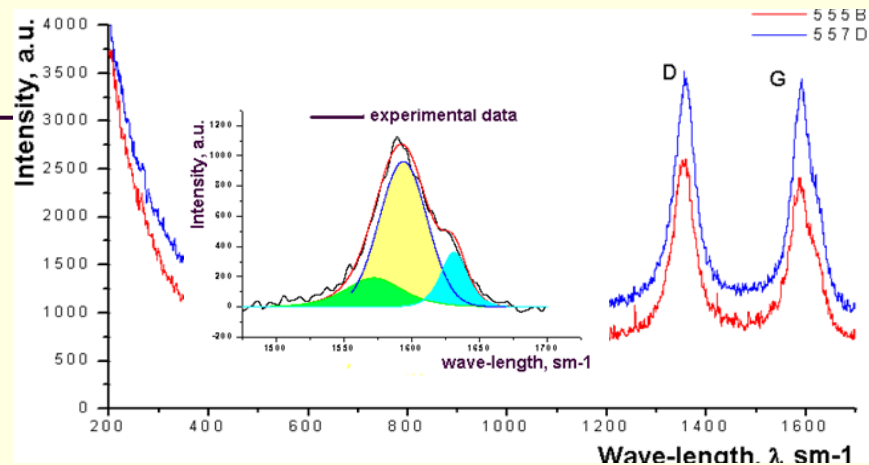
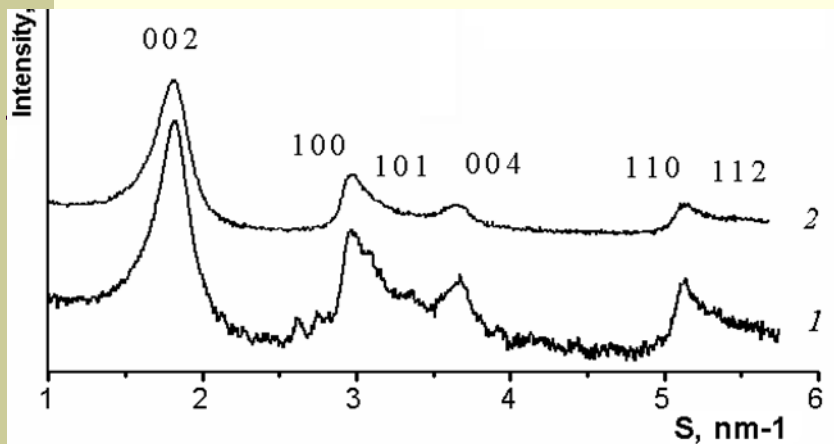


Fig. 13.1. X-ray diffraction spectra of CNT, have been obtained from ethylene (1) and propylene (2) at catalyst composition $Al_3FeMo_{0.21}$ (CoK_{α} - radiation),

$$s = \frac{4\pi \sin \theta}{\lambda}$$

Fig. 13.2. Raman spectra of MWCNT (Brucker RFS 100/s, $\lambda=514,5$ nm)

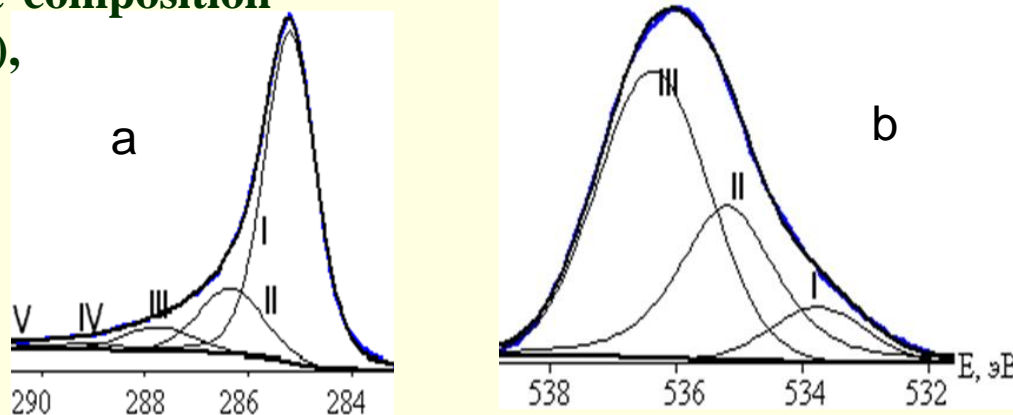
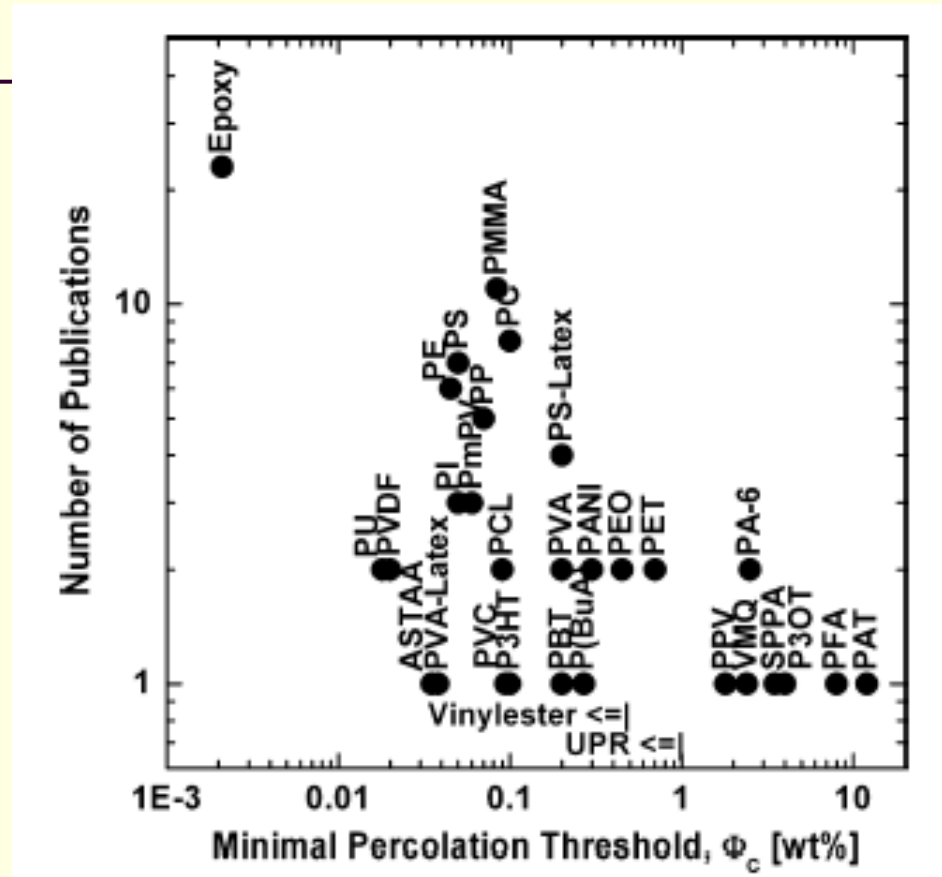
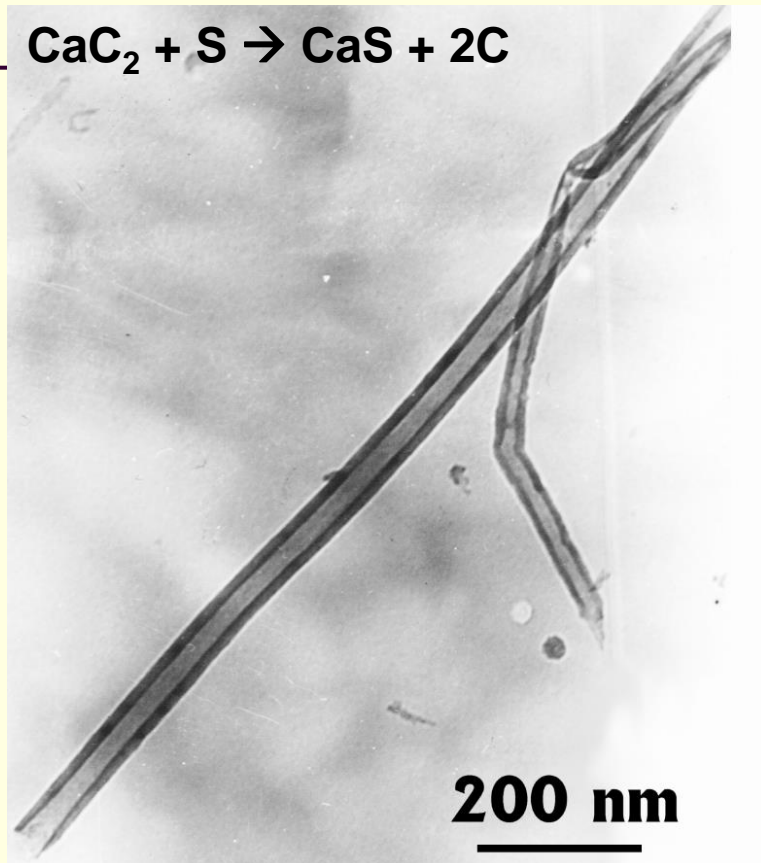


Fig 13.3. The Typical X-ray Photoelectron High Resolution Spectra of MWCNT: *a* – C 1s; *b* – O 1s. The accumulative oxygen concentration initial CNT is about 1at.%, purification CNT is about 4 at.%, chemical oxidation is about 9 at. % (SERIES 800 XPS” Kratos Analitical, MgK_{α} – 1253.6 eV)

Fig 14. Percolation Threshold in Carbon Nanotube Polymer Composites*



$$\Phi_c \approx 1/\eta; \quad \text{Aspect ration } \eta \geq 1\,000$$

*W. Bauhofer, J. Z. Kovacs. A review and analysis of electrical percolation in carbon nanotube polymer composites. Composites Science and Technology.- 2008.

Fig 15. Agglomerated CNTs synthesized in a fluidized bed reactor

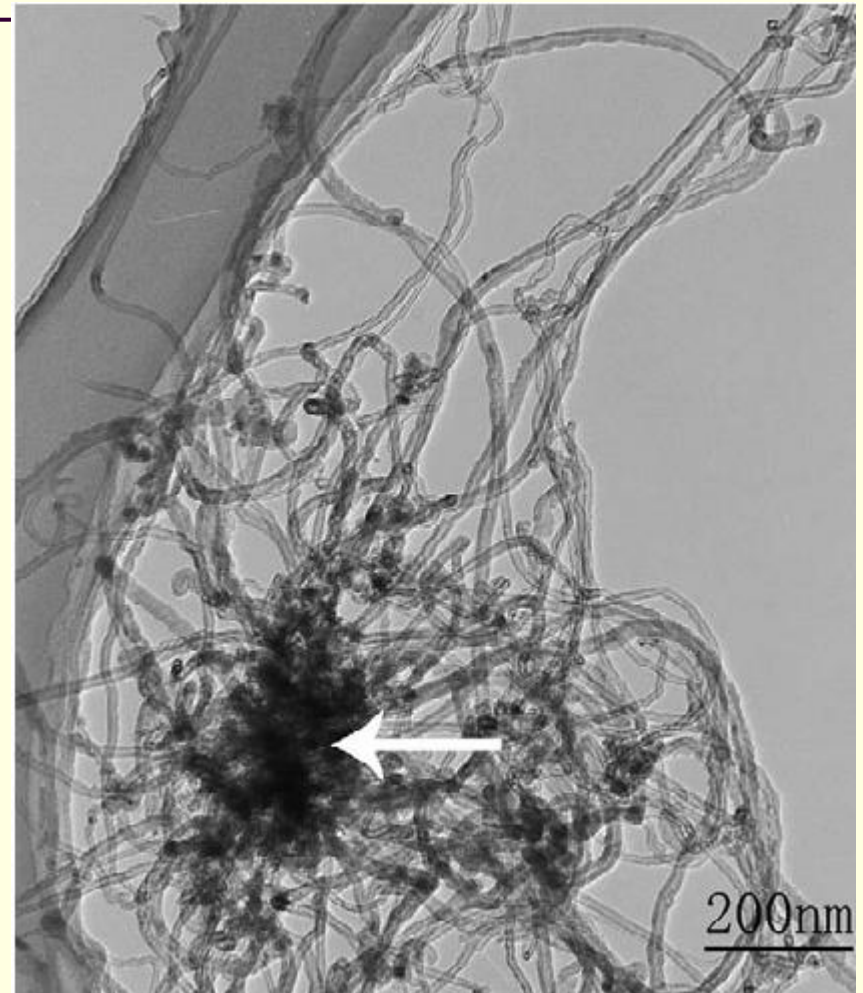
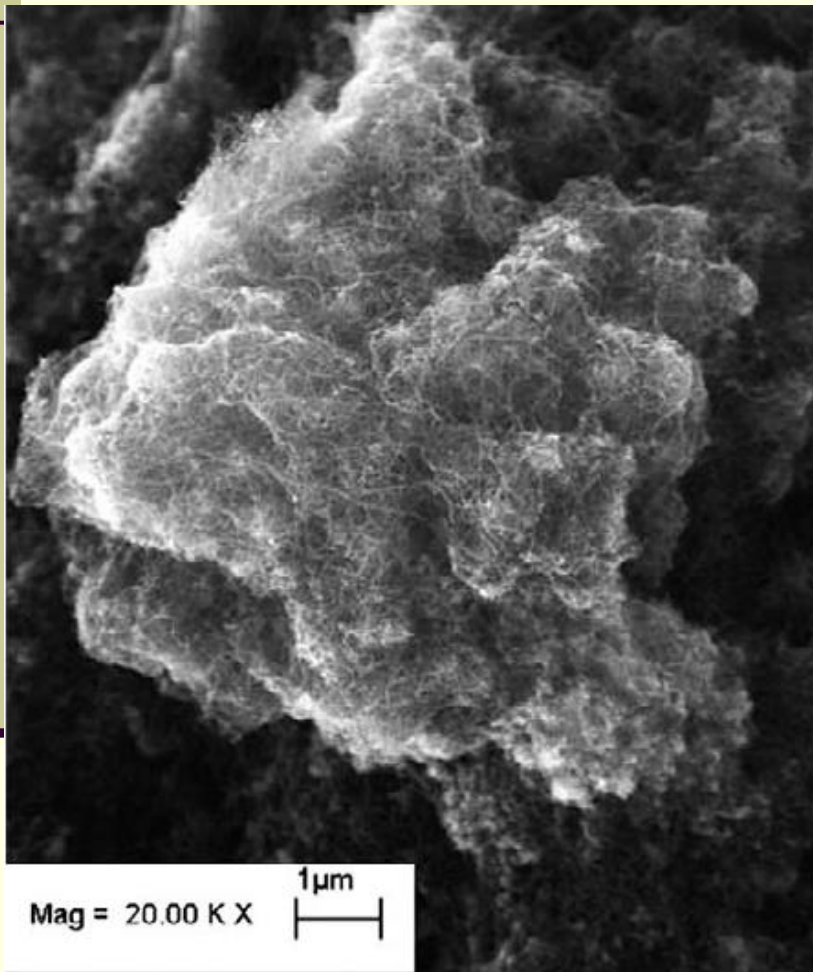


Fig. 16. Agglomerated CNTs synthesized in a fluidized bed reactor (SEM)

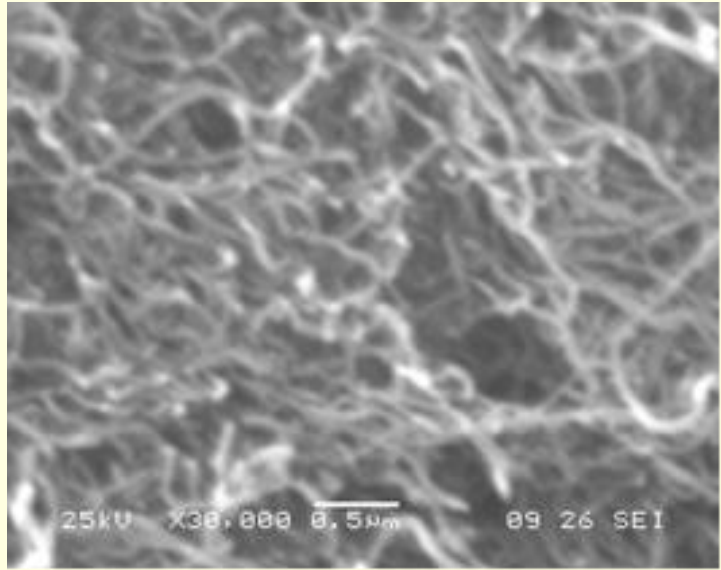
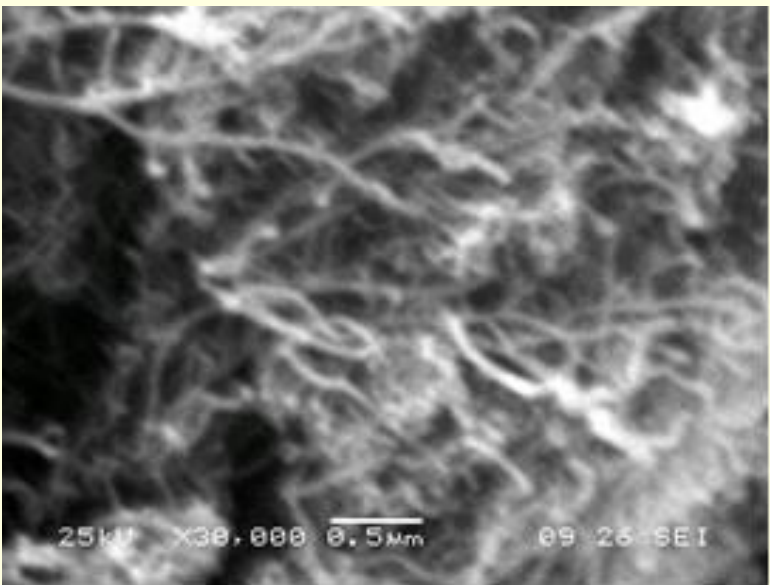
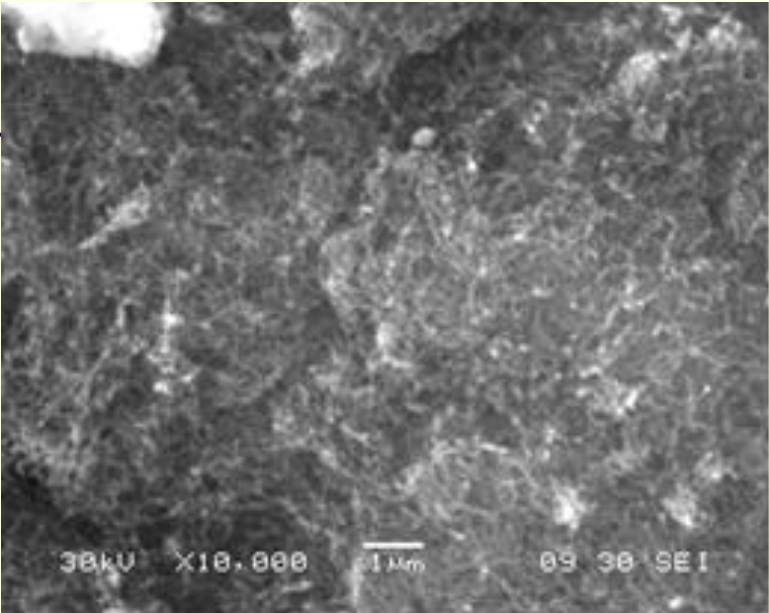
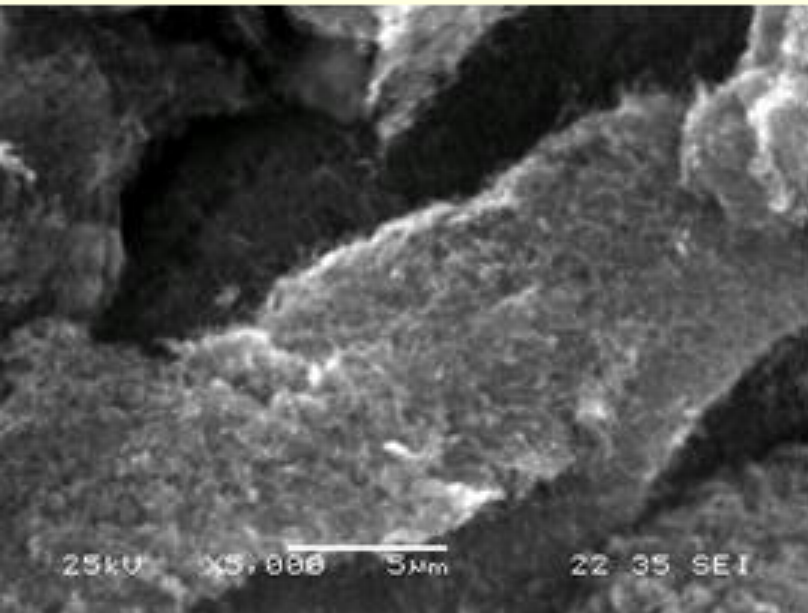


Fig. 17. Agglomerated CNTs synthesized in a fluidized bed reactor (TEM)

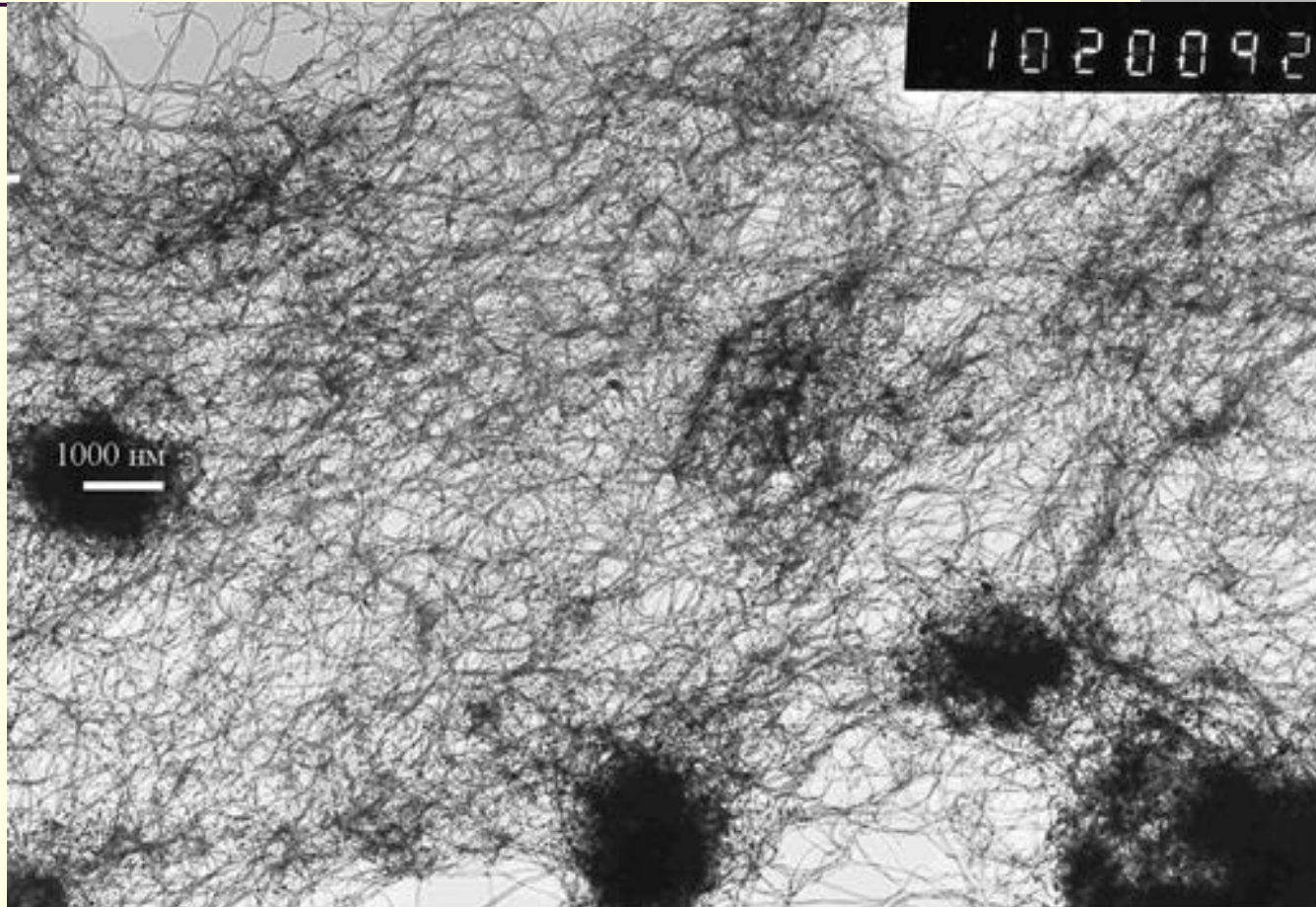
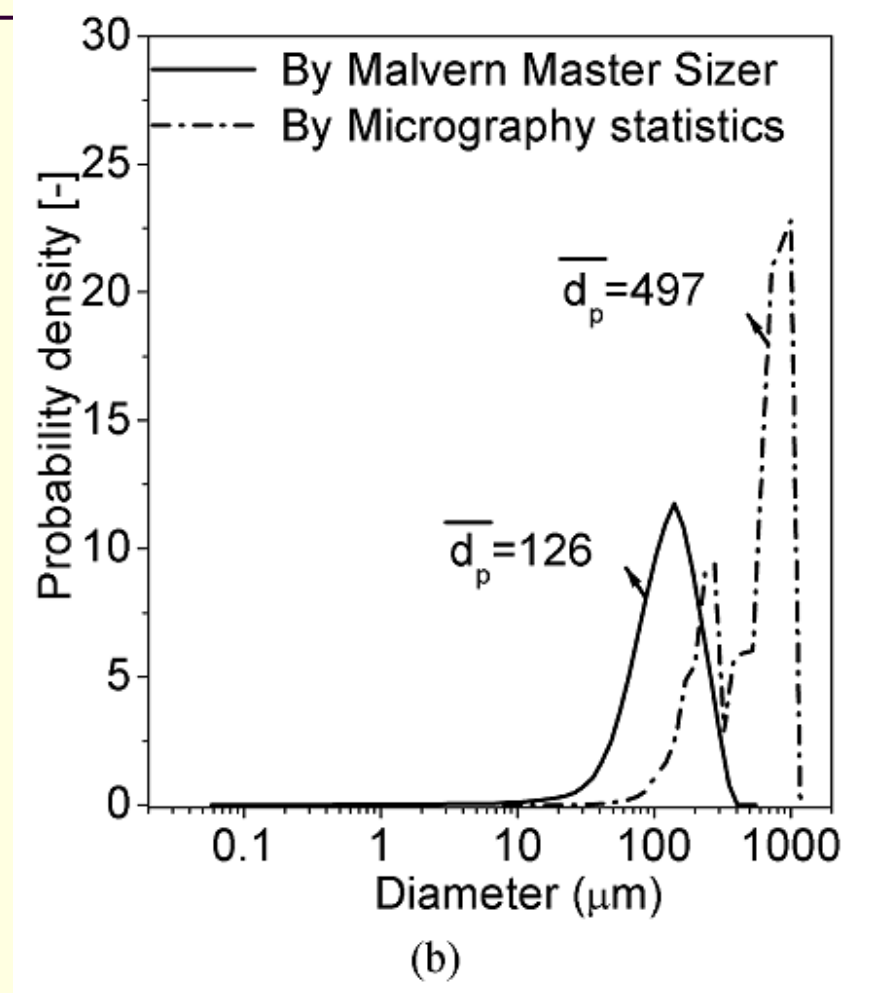
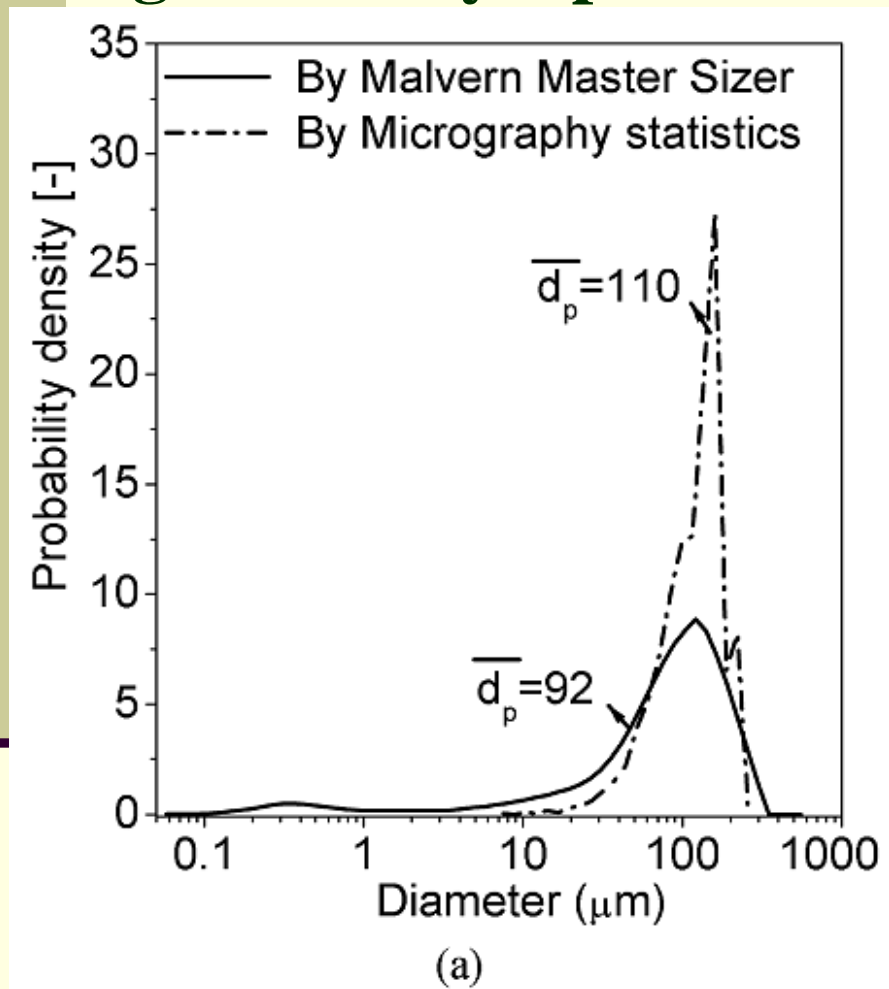
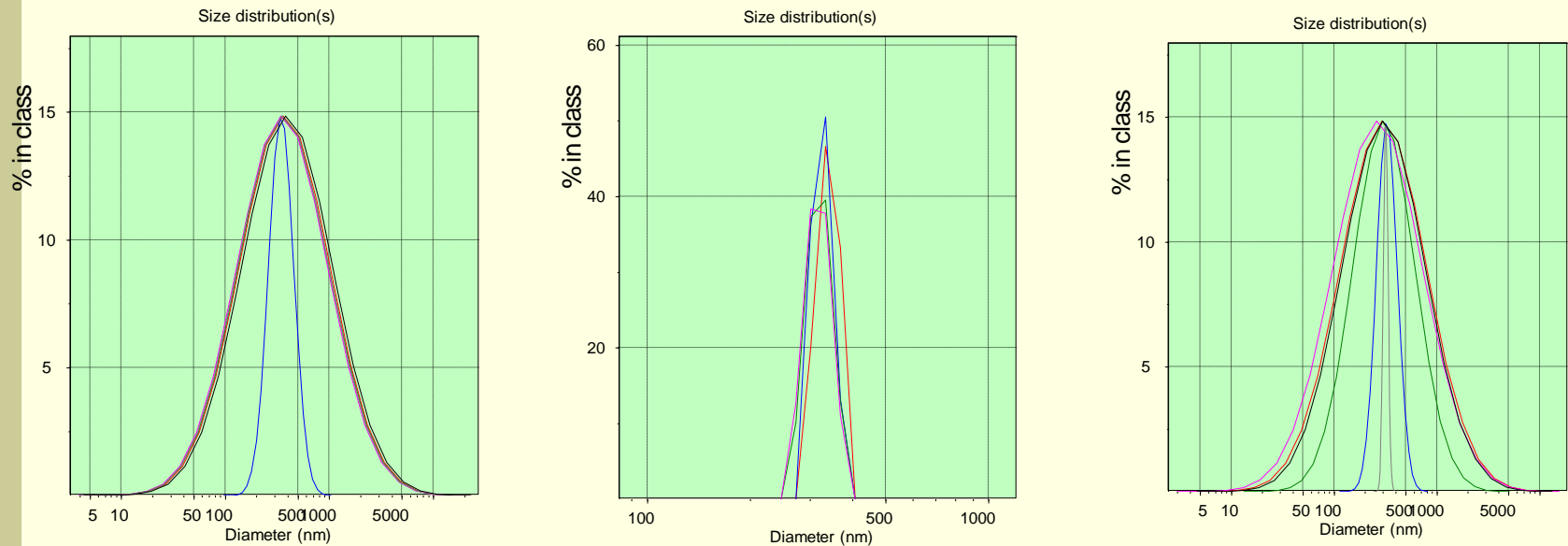


Fig. 18. Comparison of particle size measurements with laser scattering and a micrography statistical method: (a) original catalyst particles and (b) CNT agglomerates.*



* Y. Hao et al. / Carbon 41 (2003) 2855–2863

Fig. 19. Stable aqueous suspensions of MWCNTs produced in the system water-soluble polymer surfactant ions, by shear deformation and cavitation mixing



The distribution of the agglomerates size: 1 - clearly marked monodisperse distribution of nanoparticles in size from 220 to 450 nm, average size of 360 nm; 2 - to 5-fold dilution - a stable suspension with an average size of 300 nm; 3 - in the polymodal approximation it is observed fraction near 150 nm in size.

Fig. 20. Structural and physicochemical properties of polymer composites filled by MWCNT

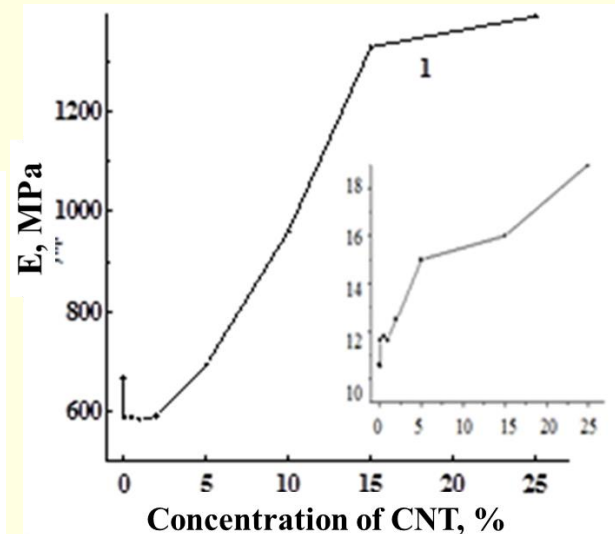
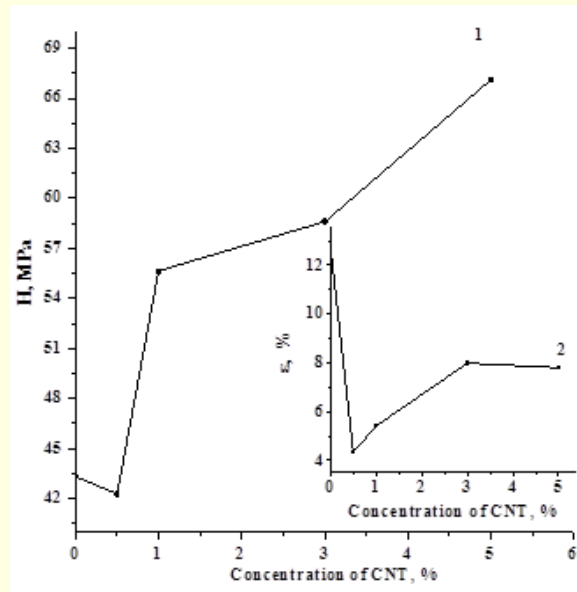
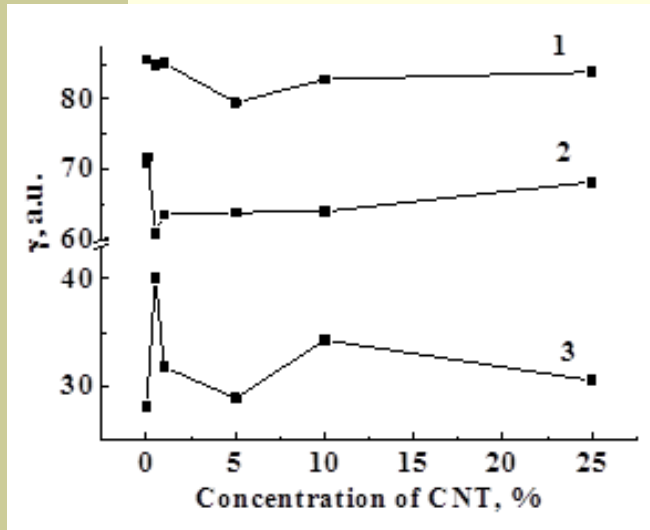


Fig. 20.1. Dependence of the degree of crystallinity of filled polymers (γ) from concentration of MWCNT: Polyethylene/ MWCNT - (1); polypropylene/ MWCNT - (2); PTFE/ MWCNT - (3).

Fig. 20.2. Dependence of breaking stress (H) – 1 and breaking deformation (ϵ) – 2 of filled polypropylene from concentration of MWCNT

Fig.20.3. Dependence of the modulus of elasticity (E) - 1 and conventional yield stress $\sigma_{0.2}$ -2 of filled PTFE from concentration of MWCNT

The compressibility and the recoverability of products from EG and system EG / 0.1% wt. MWCNT

Sample	Density , g/cm³	Compre ssibility, %%	Relative standard deviation, %	Recover- ability, %	Relative standard deviation, %
Foil EG	-	50,7	3,2	9,8	14,9
Foil EG/MWCNT	-	53,4	3,0	11,5	2,8
Packing EG	1,64	53,8	1,4	8,9	10,7
Packing EG/MWCNT	1,66	46,8	2,7	12,4	7,4

Conclusion

It is shown that the MWCNTs, along with the other matrices, are highly effective filler for carbon-carbon composite materials.

Thank you for your attention!